Improved Statistical Power with a Sparse Shape Model in Determining Aging Effect in Hippocampus and Amygdala

Moo K. Chung[1]*, Seung-Goo Kim[2], Stacey M. Schaefer[1], Carien M. van Reekum[3], Lara Peschke-Schmitz[1], Matt Sutterer[1], Richard J. Davidson[1]

[1]University of Wisconsin-Madison, USA
[2]Max Planck Institute, Germany
[3]University of Reading, UK

ABSTRACT

The sparse regression framework has been widely used in medical image processing and analysis. However, it has been rarely used in anatomical studies. We present a sparse shape modeling framework using the Laplace-Beltrami (LB) eigenfunctions of the underlying shape and show its improvement of statistical power. Traditionally, the LB-eigenfunctions are used as a basis for intrinsically representing surface shapes as a form of Fourier descriptors. To reduce high frequency noise, only the first few terms are used in the expansion and higher frequency terms are simply thrown away. However, some lower frequency terms may not necessarily contribute significantly in reconstructing the surfaces. Motivated by this idea, we present a LB-based method to filter out only the significant eigenfunctions by imposing a sparse penalty. For dense anatomical data such as deformation fields on a surface mesh, the sparse regression behaves like a smoothing process, which will reduce the error of incorrectly detecting false negatives. Hence the statistical power improves. The sparse shape model is then applied in investigating the influence of age on amygdala and hippocampus shapes in the normal population. The advantage of the LB sparse framework is demonstrated by showing the increased statistical power.

1. INTRODUCTION

There have been many basis function based shape representations such as Fourier descriptors, spherical harmonic representation,[3,11] wavelets[15] and Laplace-Beltrami eigenfunction methods.[8,10] These methods parameterize the coordinates of an object as a series expansion involving the basis functions. These basis representations do not selectively pick basis in reconstructing shapes. Usually the first few terms are used in the expansion and higher frequency terms are truncated. However, some lower frequency terms may not necessarily contribute significantly in reconstructing the shape while high frequency terms are actually important. Motivated by this simple idea, we develop a new sparse shape modeling framework that selectively filter out basis functions.

In order to show the improved performance of the propose shape representation, we introduce the statistical power analysis framework, where the minimum sample size requirement for discriminating between the groups is used a criteria for the performance. Since the statistical power has to be computed along the every point in the anatomical structure, it introduce a multiple comparisons problem.[4] Currently there is *no* anatomical study that shows how to perform the power analysis under the multiple comparisons. We show the proposed sparse shape model can improve the power by 9.1%, which is considered as significant improvement.

The proposed method is subsequently applied in characterizing gender specific aging in the hippocampus and amygdala system. The main contributions of the paper are the introductions of (1) the new sparse shape model using the intrinsic Laplace-Beltrami eigenfunctions and (2) the new power analysis framework under multiple comparisons.

Send correspondence to Moo K. Chung, 1500 Highland Ave. #281, Madison, WI. 53705, USA. E-mail: mkchung@wisc.edu. This research was supported by the grants from the National Institute of Aging (P01-AG20166) to RJD and the Vilas Associate Award from the University of Wisconsin-Madison to MKC.

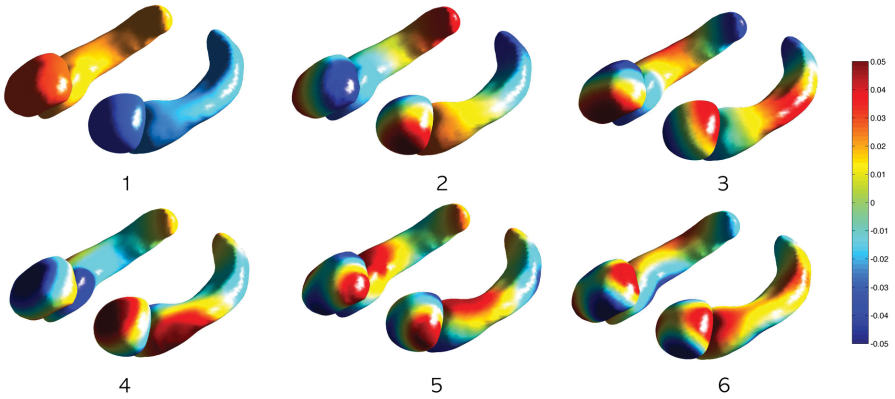

Figure 1: First six LB-eigenfunctions on amygdala and hippocampus surfaces.

2. PRILIMARY: SPARSE SHAPE REPRESENTATION

Consider a real-valued functional measurement $Y(p)$ on a manifold $\mathcal{M} \subset \mathbb{R}^3$. Y can be vectors such as surface displacement or coordinates or scalars such as length of displacement. Then we assume the following additive model:

$$Y(p) = \theta(p) + \epsilon(p), \tag{1}$$

where $\theta(p)$ is the unknown mean signal to be estimated and $\epsilon(p)$ is a zero-mean Gaussian random field. For the Laplace-Beltrami (LB) operator Δ of $\mathcal{M}$, the natural intrinsic basis functions are obtained by solving

$$\Delta\psi_j = \lambda_j\psi_j, \tag{2}$$

where the eigenfunctions ψ_j corresponding to the eigenvalues λ_j form an orthonormal basis in $L^2(\mathcal{M})$, the space of square integrable functions on $\mathcal{M}$. We may order eigenvalues as $0 = \lambda_0 \leq \lambda_1 \leq \lambda_2 \cdots$ and corresponding eigenfunctions as $\psi_0, \psi_1, \psi_2, \cdots$. Since LB-operator on an arbitrary curved surface is unknown, the eigenfunctions are numerically estimated by discretizing the LB-operator using the Cotan discretization.[2,8] The first six LB-eigenfunctions are shown in Figure 1.

Using the eigenfunctions ψ_j, we can parametrically estimate the unknown mean signal $\theta(p)$ as the Fourier expansion:

$$\widehat{\theta}(p) = \sum_{i=0}^{k} \beta_j\psi_j,$$

where β_j are the Fourier coefficients to be estimated. The Fourier coefficients can be obtained by the usual least squares estimation (LSE) by solving $\mathbf{Y} = \boldsymbol{\psi}\boldsymbol{\beta}$, where $\mathbf{Y} = (Y(p_1), \cdots, Y(p_n))'$, $\boldsymbol{\beta} = (\beta_1, \cdots, \beta_k)'$ and $\boldsymbol{\psi} = (\psi_i(p_j))$ is an $n \times k$ matrix of eigenfunctions evaluated at mesh vertices. The Fourier coefficients $\boldsymbol{\beta}$ are then estimated as

$$\widehat{\boldsymbol{\beta}} = (\boldsymbol{\psi}'\boldsymbol{\psi})^{-1}\boldsymbol{\psi}'\mathbf{Y}. \tag{3}$$

In most basis representation techniques using LB-eigenfunctions or spherical harmonics (SPHARM), only the first few terms are used in the expansion and higher frequency terms are simply thrown away to reduce the high frequency noise.[8,11] For example, between 12 and 15 degree SPHARM expansions were used for hippocampus and caudate surfaces.[11] However, some lower frequency terms may not necessarily contribute significantly in reconstructing the surfaces. Motivated by this idea, we propose to sparsely filter out insignificant eigenfunctions by imposing the additional L_1-norm penalty to sparsely filter out insignificant low degree coefficients. Following,[5] L_1-estimation is given by

$$\widehat{\boldsymbol{\beta}} = \min_{\boldsymbol{\beta}} ||\mathbf{Y} - \boldsymbol{\psi}\boldsymbol{\beta}||_2^2 + \lambda||\boldsymbol{\beta}||_1, \tag{4}$$

where the parameter $\lambda > 0$ controls the amount of sparsity. Figure 2 shows an example of the shape shape representation where surface coordinates are sparsely filtered out.

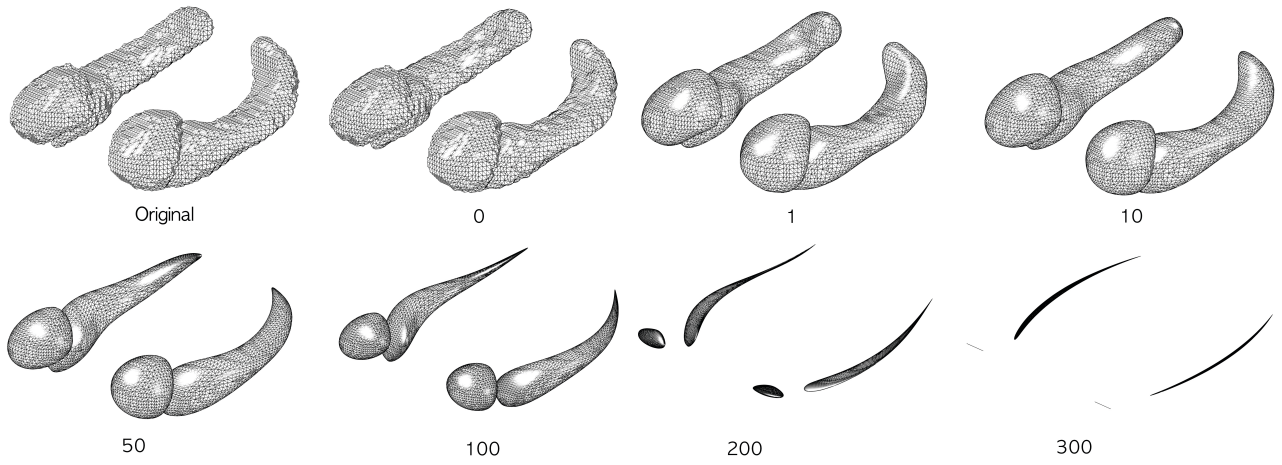

Figure 2: Sparse shape representations for different sparse parameter λ. As λ increases, the shape itself becomes sparse. For sufficiently large λ, it represents the skeleton of the underlying shape. $\lambda = 1$ is used in the study.

3. STATISTICAL POWER UNDER MULTIPLE COMPARISONS

The effect of the sparse shape model is quantified using the power analysis. Power analysis is rarely done in anatomical studies and usually did not account for interdependency of voxels.[4,6] In this paper, we show how to perform the power analysis under spatial dependency of voxels, a multiple comparisons problem. We demonstrate that the proposed model can boost the statistical power.

The usual hypotheses for testing the significance of signal in the model (1) under multiple comparisons is given by

$$H_0 : \theta(p) = 0 \text{ for all } p \in \mathcal{M} \text{ vs. } H_1 : \theta(p) > 0 \text{ for some } p \in \mathcal{M}.$$

Given a procedure for testing for the significance of θ, the type-I error (denoted as α is the probability of rejecting H_0 when H_0 is true, i.e. $\alpha = P(\text{reject } H_0 \mid H_0 \text{ true})$. On the other hand, the type-II error (denoted as β) is the probability of not rejecting H_0 when H_0 is false, i.e. $\beta = P(\text{not reject } H_0 \mid H_0 \text{ false})$. The *power* $\mathcal{P}$ of the procedure is defined as $1 - \beta$ and written as

$$\mathcal{P} = P(\text{reject } H_0 \mid H_1 \text{ true}).$$

The power is the probability of rejecting the null hypothesis that there is no signal when there is an actual signal. *When the test procedure has the power of 0.9, it implies that the method can correctly detect signal* 90% *of time when there is a real signal.* Statistical power is somewhat similar to classification accuracy in machine learning. The power is usually given in as a function of sample size. With the infinite number of samples, we can then achieve 100% power with any method. The statistical power is a good summary measure for numerically evaluating the performance of a method although it is rarely used in this fashion due to the difficulty of computing it under multiple comparisons.

Power under Multiple Comparisons. To compute the power over manifold $\mathcal{M}$, it is necessary to determine the type-I error first. Given a test random field $T(p)$, we reject H_0 if $T(p) > h$ for some thresholding h for all $p \in \mathcal{M}$. This is equivalent to the event $\sup_{p\in\mathcal{M}} T(p) > h$.[4] Hence, the type-I error over $\mathcal{M}$ is given by

$$\alpha = P\Big(\sup_{p\in\mathcal{M}} T(p) > h\Big).$$

The rejection region is taken as the subset of $\mathcal{M}$ (Figure 3):

$$\mathcal{M}_1 = \{x \in \mathcal{M} | T(x) > h\}.$$

Then the over all statistical power $\mathcal{P}$ is computed as

$$\mathcal{P} = P\Big(\sup_{t\in\mathcal{M}} T(t) > h \Big| H_1\Big). \tag{5}$$

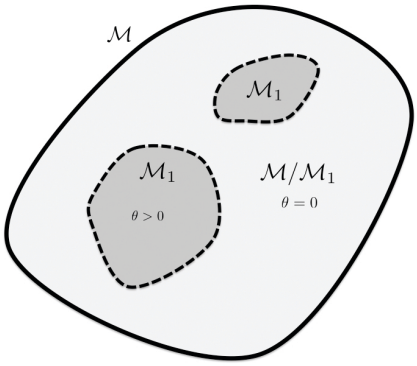

Figure 3: Under H_1, there exists nonempty rejection regions $\mathcal{M}_1$ where the signal is significant.

4. EXPERIMENTAL RESULTS

As the part of ongoing study on midlife in the US,,[13] we have high-resolution T1-weighted inverse recovery fast gradient echo MRI, collected in 124 contiguous 1.2-mm axial slices (TE=1.8 ms; TR=8.9 ms; flip angle = 10°; FOV = 240 mm; 256 × 256 data acquisition matrix) of 69 middle-age and elderly adults ranging between 38 to 79 years (mean age = 58.0 ± 11.4 years). There are 23 men and 46 women in the study. Trained raters manually segmented amygdala and hippocampus. Then we performed a nonlinear image registration using the diffeomorphic shape and intensity averaging technique with the cross-correlation as the similarity metric through Advanced Normalization Tools (ANTS).[1] An initial template was constructed from a random subsample of 10 subjects. Using the deformation field obtained from warping the individual image to the template, we aligned the amygdala and hippocampus binary masks to the template space. The normalized masks were then averaged to produce the final study template. The isosurface of the template was extracted using the marching cube algorithm.[7] The displacement vector field is defined on each voxel, while the vertices of mesh are located within a voxel. So we linearly interpolated the vector field on mesh vertices from the voxels.

Sparse Shape Analysis. The length of displacement vector field along the template surface was estimated using the sparse framework with $\lambda = 1$ and $k = 1000$ eigenfunctions. This is sufficient number of basis functions. Only 5% of largest coefficients are used in the sparse representation. This has an effect of smoothing out noisy displacement. The age effect on the displacement length is regressed over the total brain volume and other variables:

$$\texttt{length} = \beta_1 + \beta_2 \cdot \texttt{brain} + \beta_3 \cdot \texttt{age} + \beta_4 \cdot \texttt{gender} + \epsilon, \tag{6}$$

where ϵ is a zero mean Gaussian field. The age effect was determined by performing T-test on the parameter β_3. The results are displayed in Figure 4. We found the regions of highly significant effect of age on the posterior part of hippocampi (corrected p-value < 0.05). Particularly on the caudal regions of the left and right hippocampi, we found highly localized age effect. It is consistent with other shape modeling studies on hippocampus.[9,14] We did not find any age effects on the amygdala surface.

Power Computation by Resampling. The direct power computation using the random field theory requires estimating the smoothness of signal, which is not trivial.[4] Instead we propose a resampling technique. First, we need to identify the threshold h corresponding to a specific α-level. For T-random field $T(x)$, the threshold h corresponding to the type-I error at 0.05 is given by

$$P\Big(\sup_{x\in\mathcal{M}} T(x) > h\Big) = 0.05,$$

where $\mathcal{M}$ is the surface of interest. For the power computation, it is needed to identify the rejection region $\mathcal{M}_1$ as well. The rejection region is taken as the subset of $\mathcal{M}$:

$$\mathcal{M}_1 = \{x \in \mathcal{M} | T(x) > h\}.$$

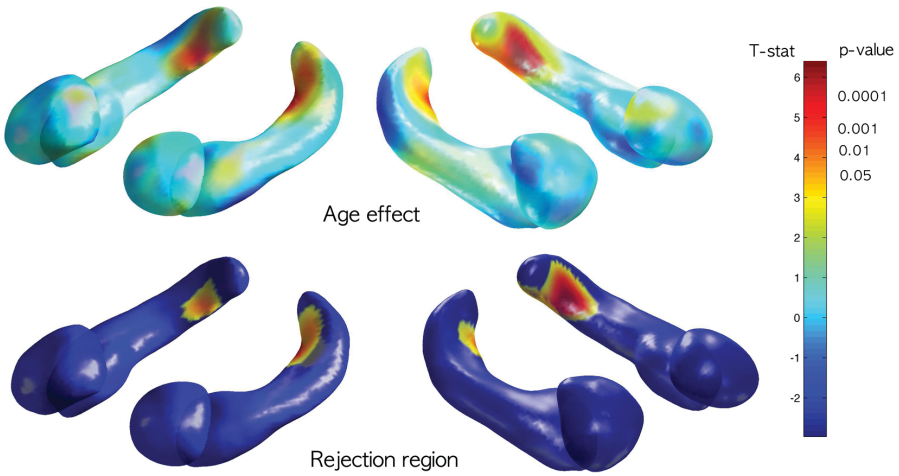

Figure 4: Age effect on hippocampi. The T-stat. and the corrected p-value are shown. There is no age effect on amygdale. Rejection regions $\mathcal{M}_1$ corresponding to 0.05 level are also shown.

Then the over all statistical power $\mathcal{P}$ is computed as

$$\mathcal{P} = P\Big(\sup_{x\in\mathcal{M}_1} T(x) > h\Big),$$

where the supremum is restricted to the rejection region $\mathcal{M}_1$ (Figure 4). The thresholds h corresponding to $\alpha = 0.05$ for the left and right hippocampi are 3.71 and 3.77. The resampling based power computation is performed as follows.

(1) Set the counter $c = 0$.

(2) Randomly pick n subjects out of total 69 subjects.

(3) For n subjects, perform GLM (6) and obtain the t-statistic values in $\mathcal{M}_1$.

(4) If any t-static value is larger than h, increase the counter $c \leftarrow c + 1$.

(5) Repeat the above procedures $m = 5000$ times.

The frequency of rejection c/m approximates the power $\mathcal{P}$ as m becomes large for the given sample size n. 5000 resamples are sufficient to guarantee the robust estimation of the power. The resulting power is plotted as a function of sample size (Figure 5). In the right hippocampus, we have increase of 0.091 in statistical power at the sample size 50. This implies the proposed sparse model can increase the accuracy of detection by up to 9.1% in smaller sample studies.

5. CONCLUSION

We have presented a new sparse shape modeling framework using the Laplace-Beltrami eigenfunctions. The proposed framework is demonstrated to increase the statistical power by up to 9.1%. The significant structural changes found on hippocampi due to normal aging is consistent with the previous hippocampus shape analyses.[9,12]

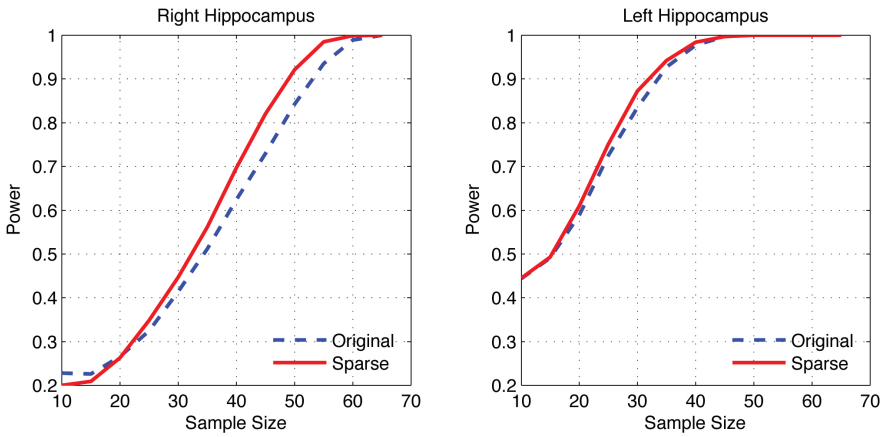

Figure 5: Statistical power over sample size computed under multiple comparisons. The sparse regression increases statistical power.

REFERENCES

1. B.B. Avants, C.L. Epstein, M. Grossman, and J.C. Gee. Symmetric diffeomorphic image registration with cross-correlation: Evaluating automated labeling of elderly and neurodegenerative brain. *Medical image analysis*, 12:26–41, 2008.
2. M.K. Chung. *Statistical Morphometry in Neuroanatomy*. Ph.D. Thesis, McGill University, 2001.
3. M.K. Chung, R. Hartley, K.M. Dalton, and R.J. Davidson. Encoding cortical surface by spherical harmonics. *Satistica Sinica*, 18:1269–1291, 2008.
4. S. Hayasaka, A.M. Peiffer, C.E. Hugenschmidt, and P.J. Laurienti. Power and sample size calculation for neuroimaging studies by non-central random field theory. *NeuroImage*, 37:721–730, 2007.
5. S.J. Kim, K. Koh, M. Lustig, S. Boyd, and D. Gorinevsky. An interior-point method for large-scale l1-regularized least squares. *IEEE Journal of Selected Topics in Signal Processing*, 1:606–617, 2007.
6. J. P. Lerch and A.C. Evans. Cortical thickness analysis examined through power analysis and a population simulation. *NeuroImage*, 24:163–173, 2005.
7. W.E. Lorensen and H.E. Cline. Marching cubes: A high resolution 3D surface construction algorithm. In *Proceedings of the 14th annual conference on Computer graphics and interactive techniques*, pages 163–169, 1987.
8. A. Qiu, D. Bitouk, and M.I. Miller. Smooth functional and structural maps on the neocortex via orthonormal bases of the laplace-beltrami operator. *IEEE Transactions on Medical Imaging*, 25:1296–1396, 2006.
9. A. Qiu and M.I. Miller. Multi-structure network shape analysis via normal surface momentum maps. *NeuroImage*, 42:1430–1438, 2008.
10. S. Seo, M.K. Chung, and H.K. Vorperian. Heat kernel smothing using laplace-beltrami eigenfunctions. In *Medical Image Computing and Computer-Assisted Intervention – MICCAI 2010*, volume 6363 of *Lecture Notes in Computer Science*, pages 505–512, 2010.
11. M. Styner, I. Oguz, S. Xu, C. Brechbuhler, D. Pantazis, J. Levitt, M. Shenton, and G. Gerig. Framework for the statistical shape analysis of brain structures using spharm-pdm. In *Insight Journal, Special Edition on the Open Science Workshop at MICCAI*, 2006.
12. P.M. Thompson, K.M. Hayashi, G. de Zubicaray, A.L. Janke, S.E. Rose, J. Semple, M.S. Hong, D.H. Herman, D. Gravano, D.M. Doddrell, and A.W. Toga. Mapping hippocampal and ventricular change in alzheimer disease. *NeuroImage*, 22:1754–1766, 2004.
13. C.M. Van Reekum, S.M. Schaefer, R.C. Lapate, C.J. Norris, L.L. Greischar, and R.J. Davidson. Aging is associated with positive responding to neutral information but reduced recovery from negative information. *Social Cognitive and Affective Neuroscience*, 6:177–185, 2011.
14. Y. Xu, D.J. Valentino, A.I. Scher, I. Dinov, L.R. White, P.M. Thompson, L.J. Launer, and A.W. Toga. Age effects on hippocampal structural changes in old men: the haas. *NeuroImage*, 40:1003–1015, 2008.
15. P. Yu, P.E. Grant, Y. Qi, X. Han, F. Segonne, R. Pienaar, E. Busa, J. Pacheco, N. Makris, R.L. Buckner, et al. Cortical Surface Shape Analysis Based on Spherical Wavelets. *IEEE Transactions on Medical Imaging*, 26:582, 2007.